Closed Form Expression for the Vibration Problem of a Transversely Isotropic Magneto-Electro-Elastic Plate

Mei-Feng Liu
Associate Professor
Department of Applied Mathematics,
I-Shou University,
Dashu Township,
Kaohsiung County 840, Taiwan, R.O.C.

Tai-Ping Chang
Professor
Department of Construction Engineering,
National Kaohsiung First University of Science and Technology,
Kaohsiung 811, Taiwan, R.O.C.

A closed form expression for the transverse vibration of a magnetoelectroelastic (MEE) thin plate is derived, and the exact solution for the free vibration of a two-layered $BaTiO_3-CoFe_2O_4$ composite is obtained. Based on the Kirchhoff thin plate theory, the bending problem of a transversely isotropic MEE rectangular plate is investigated, and the governing equation in terms of the transverse displacement is then presented in a rather compact form. The material coefficients for such MEE plate are expressed uniquely by the volume fraction (vf) of the two-layered $BaTiO_3-CoFe_2O_4$ composite, which indicates a transversely isotropic MEE medium. The natural frequencies of such MEE plate are evaluated analytically, and the effects of different volume fractions on the natural frequency are further discussed.
[DOI: 10.1115/1.3176996]

1 Introduction

The dynamical responses of elastic bodies under various external conditions have drawn significant attentions and researches by many professional engineers and scientists. Above all, the vibration analysis of a thin plate with or without piezoelectric effects has been fully carried out. Since piezoelectric structure has the capability to transfer either mechanical strains into electric signals or vice versa, the investigations of such electroelastic coupling have been completely performed in the last decades. Recently, the so-called magnetoelectroelastic (MEE) composite has been vigorously discussed due to its multiphase properties including elasticity, electricity, and magnetism, as well as the interactions among them. The MEE composites are normally made of the combinations between piezoelectric and piezomagnetic components and have found increasing values especially in making efficient sensors and actuators for smart and intelligent structures or systems. MEE solids can be treated as an extension for the piezoelectric medium by further taking into account the interactive behaviors on elastic magnetism and electromagnetism on the structure, respectively. The MEE material does not only possess the ability to convert energy among magnetism, electricity, or elasticity into another form but also exhibits a magnetoelectric effect that does not appear in a single-phase piezoelectric or piezomagnetic material. In some cases, the magnetoelectric effect of piezoelectric/piezomagnetic composites can even be obtained a hundred times larger than that of a single-phase magnetoelectric material [1]. Since MEE material are extensively used as magnetic field probes, electric packing, acoustic, hydrophones, medical ultrasonic imaging, sensors, and actuators, with the responsibility of magneto-electromechanical energy conversion, it is valuable to establish a more compact and systematic form for the medium, which can be used widely.

Li [1] studied the average MEE fields in a multi-inclusion or inhomogeneity that is embedded in an infinite matrix, and estimated the effective MEE moduli of piezoelectric-piezomagnetic composites for both $BaTiO_3$ fiber reinforced $CoFe_2O_4$ and $BaTiO_3-CoFe_2O_4$ laminates. It has been shown that the magnetoelectro coupling demonstrated by magnetoelectro coefficients vary with the volume faction of $BaTiO_3$ and have opposite signs for fibrous and laminated composites, respectively. Pan [2] obtained the exact solution for three-dimensional, anisotropic, linear MEE, simply-supported, and multilayered rectangular plates under static loadings. It is stated that even for a relatively thin plate, responses from an internal load are quite different from those on the surface load. Aboudi [3] performed the micromechanical analysis for fully coupled electromagnetothermalelastic composites by employing the homogenization micromechanical method, and predicted the effective moduli of a fibrous composite with various values of volume fraction, which represents the volume ratio between $CoFe_2O_4$ and $BaTiO_3$. Analytical solutions are derived by Pan and Heyliger [4] for free vibrations of three-dimensional, anisotropic, linear MEE, and multilayered rectangular plates under simply-supported conditions. The typical natural frequencies and mode shapes are presented for both single homogeneous plates and sandwich piezoelectric/piezomagnetic plates. Wang and Shen [5] extended their previous works on piezoelectric media to study the general solution of three-dimensional problems in a transversely isotropic MEE media through five newly introduced potential functions. Chen et al. [6] established a micromechanical model to evaluate the effective properties of a layered composite with piezoelectric and piezomagnetic components. In their study, numerical results for a $BaTiO_3-CoFe_2O_4$ composite with 2–2 connectivities are obtained, and the dependences of MEE coefficients, which are the so-called product properties of the composite on the volume fraction of $BaTiO_3$, are clearly depicted. A boundary integral formulation for the plane problem of MEE media are performed by Haojiang and Aimin [7] using a strict differential operator theory. They obtained the fundamental solutions for an infinite MEE plane in terms of four harmonic functions, which satisfied a set of reduced second order partial differential equation for distinct eigenvalue cases. Guan and He [8] derived the fundamental equation for the plane problem of a transversely isotropic MEE media by applying the Almansi's theorem, and expressed all physical quantities by four harmonic functions for distinct and nondistinct cases. Chen et al. [9] presented novel state space formulations for the static problem of transversely isotropic thermomagnetoelectroelastic materials by virtue of a separation technique. The free vibration investigation was recently performed by Ramirez et al. [10], who found that some natural frequencies of a multifield (piezoelectric/magnetostrictive) plate were identical to the ones of the corresponding elastic plate. They argued that certain vibration modes of the plate were insensitive to the coupling effects among elastic, electric, and magnetic fields.

In this paper, the bending problem for a transversely isotropic MEE rectangular plate is analyzed by imposing the Kirchhoff thin plate hypothesis on the plate constituent. The governing equation in terms of the transverse displacement of the plate is derived, and a rather compact form indicating the multiple effects between elasticity, electricity, and magnetism of the plate is presented successfully for the first time. The material coefficients for such MEE

Contributed by the Applied Mechanics Division of ASME for publication in the Journal of Applied Mechanics. Manuscript received November 6, 2008; final manuscript received June 3, 2009; published online December 9, 2009. Review conducted by Wei-Chau Xie.

plate can be expressed uniquely by introducing the so-called volume fraction of the two-layered $BaTiO_3-CoFe_2O_4$ composite, which represents the ratio of fiber material $BaTiO_3$ to matrix material $CoFe_2O_4$ for a transversely isotropic MEE medium. The natural frequencies of such MEE plate is evaluated through the formulation mentioned in this study, which are compared with the data obtained by previous research works, and the discrepancies have been discussed.

2 Formulations

Let us consider a transversely isotropic MEE medium in a Cartesian coordinate system (x,y,z). If the z-axis is normal to the plane of isotropy, the constitutive equations are, according to Ref. [9]

$$\sigma_x = c_{11}\frac{\partial u}{\partial x} + c_{12}\frac{\partial v}{\partial y} + c_{13}\frac{\partial w}{\partial z} + e_{31}\frac{\partial \phi}{\partial z} + q_{31}\frac{\partial \psi}{\partial z}$$

$$\sigma_y = c_{12}\frac{\partial u}{\partial x} + c_{11}\frac{\partial v}{\partial y} + c_{13}\frac{\partial w}{\partial z} + e_{31}\frac{\partial \phi}{\partial z} + q_{31}\frac{\partial \psi}{\partial z}$$

$$\sigma_z = c_{13}\frac{\partial u}{\partial x} + c_{13}\frac{\partial v}{\partial y} + c_{33}\frac{\partial w}{\partial z} + e_{33}\frac{\partial \phi}{\partial z} + q_{33}\frac{\partial \psi}{\partial z}$$

$$\tau_{xz} = c_{44}\left(\frac{\partial u}{\partial z} + \frac{\partial w}{\partial x}\right) + e_{15}\frac{\partial \phi}{\partial x} + q_{15}\frac{\partial \psi}{\partial x}$$

$$\tau_{yz} = c_{44}\left(\frac{\partial v}{\partial z} + \frac{\partial w}{\partial y}\right) + e_{15}\frac{\partial \phi}{\partial y} + q_{15}\frac{\partial \psi}{\partial y}$$

$$\tau_{xy} = c_{66}\left(\frac{\partial u}{\partial y} + \frac{\partial v}{\partial x}\right)$$

$$D_x = e_{15}\left(\frac{\partial u}{\partial z} + \frac{\partial w}{\partial x}\right) - \varepsilon_{11}\frac{\partial \phi}{\partial x} - d_{11}\frac{\partial \psi}{\partial x} \tag{1}$$

$$D_y = e_{15}\left(\frac{\partial v}{\partial z} + \frac{\partial w}{\partial y}\right) - \varepsilon_{11}\frac{\partial \phi}{\partial y} - d_{11}\frac{\partial \psi}{\partial y}$$

$$D_z = e_{31}\frac{\partial u}{\partial x} + e_{31}\frac{\partial v}{\partial y} + e_{33}\frac{\partial w}{\partial z} - \varepsilon_{33}\frac{\partial \phi}{\partial z} - d_{33}\frac{\partial \psi}{\partial z}$$

$$B_x = q_{15}\left(\frac{\partial u}{\partial z} + \frac{\partial w}{\partial x}\right) - d_{11}\frac{\partial \phi}{\partial x} - \mu_{11}\frac{\partial \psi}{\partial x} \tag{2}$$

$$B_y = q_{15}\left(\frac{\partial v}{\partial z} + \frac{\partial w}{\partial y}\right) - d_{11}\frac{\partial \phi}{\partial y} - \mu_{11}\frac{\partial \psi}{\partial y}$$

$$B_z = q_{31}\frac{\partial u}{\partial x} + q_{31}\frac{\partial v}{\partial y} + q_{33}\frac{\partial w}{\partial z} - d_{33}\frac{\partial \phi}{\partial z} - \mu_{33}\frac{\partial \psi}{\partial z} \tag{3}$$

where σ_i and τ_{ij} are the normal and shear stresses; u, v, and w are the components of the mechanical displacement in x-, y-, and z-directions, respectively; ϕ, ψ, D_i, and B_i are the electric potential, magnetic potential, electric displacement components, and magnetic induction components, respectively; c_{ij}, ε_{ij}, e_{ij}, q_{ij}, d_{ij}, and μ_{ij} are the elastic, dielectric, piezoelectric, piezomagnetic, magnetoelectric, and magnetic constants, respectively. It should be noted that the relation $c_{11}=c_{12}+2c_{66}$ holds for any transversely isotropic material under consideration. In this paper, all the material parameters mentioned above are assumed to be constant. If no change density and magnetic field is applied, the equations of motion are stated as follows:

$$\frac{\partial \sigma_x}{\partial x} + \frac{\partial \tau_{xy}}{\partial y} + \frac{\partial \tau_{xz}}{\partial z} = \rho\frac{\partial^2 u}{\partial t^2}$$

$$\frac{\partial \tau_{xy}}{\partial x} + \frac{\partial \sigma_y}{\partial y} + \frac{\partial \tau_{yz}}{\partial z} = \rho\frac{\partial^2 v}{\partial t^2}$$

$$\frac{\partial \tau_{xz}}{\partial x} + \frac{\partial \tau_{yz}}{\partial y} + \frac{\partial \sigma_z}{\partial z} = \rho\frac{\partial^2 w}{\partial t^2} \tag{4}$$

$$\frac{\partial D_x}{\partial x} + \frac{\partial D_y}{\partial y} + \frac{\partial D_z}{\partial z} = 0 \tag{5}$$

$$\frac{\partial B_x}{\partial x} + \frac{\partial B_y}{\partial y} + \frac{\partial B_z}{\partial z} = 0 \tag{6}$$

where ρ is the density of the material. By utilizing the technique of separation of the variables in Eq. (4), the solution can be expressed in the form of $\mathbf{u}(x,y,z;t)=\mathbf{u}(x,y,z)e^{i\omega t}$, where $\mathbf{u}(x,y,z) =[u(x,y,z)v(x,y,z)w(x,y,z)]^t$ represents the displacement in the x, y, and z-axes, and $e^{i\omega t}$ represents a harmonic time-dependent motion.

Suppose the thickness of a MEE plate is smaller in one order of magnitude than the span or diameter of the plate, i.e., the so-called thin plate is considered, the fundamental Kirchhoff hypothesis for the small-deflection theory of a simple bending problem can be applied, and the following assumptions [11,12] are adopted for the present analysis.

(i) The deflection of the midsurface is small compared with the thickness of the plate. The slope of the deflected surface is, therefore, very small, and the square of the slope is a negligible quantity in comparison with unity.
(ii) The midplane remains unstrained subsequent to bending.
(iii) Plane sections initially normal to the midsurface remain plane and normal to that surface after the bending. This means that the vertical shear strains γ_{xz} and γ_{yz} are negligible. The deflection of the plate is thus associated principally with bending strains. It is deduced, therefore, that the normal strain ε_z, resulting from transverse loading, may also be omitted.
(iv) The stress normal to the midplane σ_z is small compared with the other stress components, and may be neglected. This supposition becomes unreliable in the vicinity of highly concentrated transverse loads.

As a consequence of assumption (iii), the strain-displacement relations can be reduced into

$$\varepsilon_x = \frac{\partial u}{\partial x}, \quad \varepsilon_y = \frac{\partial v}{\partial y}, \quad 2\varepsilon_{xy} = \gamma_{xy} = \frac{\partial u}{\partial y} + \frac{\partial v}{\partial x} \tag{7}$$

$$\varepsilon_z = \frac{\partial w}{\partial z} = 0, \quad 2\varepsilon_{xz} = \gamma_{xz} = \frac{\partial w}{\partial x} + \frac{\partial u}{\partial z} = 0$$

$$2\varepsilon_{yz} = \gamma_{yz} = \frac{\partial w}{\partial y} + \frac{\partial v}{\partial z} = 0 \tag{8}$$

where $\gamma_{ij}=\gamma_{ji}$ $(i,j=x,y,z)$ represents the mechanical strains. After integrating Eq. (1), we can obtain

$$w = w(x,y) \tag{9}$$

which indicates that the lateral deflection does not vary over the plate thickness. In the same manner, integration of expressions for γ_{xz} and γ_{yz} gives

$$u = -z\frac{\partial w}{\partial x} + u_0(x,y), \quad v = -z\frac{\partial w}{\partial y} + v_0(x,y) \tag{10}$$

Base on assumption (ii) in the last paragraph, we may conclude that $u_0=v_0=0$. Thus, we have

$$u = -z\frac{\partial w}{\partial x}, \quad v = -z\frac{\partial w}{\partial y} \tag{11}$$

It should be noted that equations in Eq. (11) are equivalent to the kinematics in the well-known classical plate theory (CPT), and which are consistent with assumption III. Substitution of Eq. (11) into Eq. (7) yields the following results:

$$\varepsilon_x = -z\frac{\partial^2 w}{\partial x^2}, \quad \varepsilon_y = -z\frac{\partial^2 w}{\partial y^2}, \quad \gamma_{xy} = -2z\frac{\partial^2 w}{\partial x\,\partial y} \tag{12}$$

The above formulas provide the strains at any point in the plate. As stated in Ref. [13], if the MEE plate is thin, the transverse shear deformations and rotary inertias can be neglected; the transverse shear strains are also negligible. In addition, the in-plane electric fields and magnetic fields can be ignored, i.e., $E_x = E_y = 0$ and $H_x = H_y = 0$. This means that only the transverse electric E_3 and magnetic field H_3 are considered in the present study. According to Maxwell's equations, these two fields are related to the electric potential ϕ and magnetic potential ψ by the following relations:

$$E_x = -\frac{\partial \varphi}{\partial x} = 0, \quad E_y = -\frac{\partial \phi}{\partial y} = 0, \quad E_z = -\frac{\partial \phi}{\partial z} \tag{13}$$

$$H_x = -\frac{\partial \psi}{\partial x} = 0, \quad H_y = -\frac{\partial \psi}{\partial y} = 0, \quad H_z = -\frac{\partial \psi}{\partial z} \tag{14}$$

Substituting Eqs. (7), (8), and (12)–(14) into the constitute Eqs. (1)–(3), one can obtain the reduced extended traction vectors [2] as stated below

$$\sigma_x = c_{11}\left(-z\frac{\partial^2 w}{\partial x^2}\right) + c_{12}\left(-z\frac{\partial^2 w}{\partial y^2}\right) + e_{31}\frac{\partial \varphi}{\partial z} + q_{31}\frac{\partial \psi}{\partial z}$$

$$\sigma_y = c_{12}\left(-z\frac{\partial^2 w}{\partial x^2}\right) + c_{11}\left(-z\frac{\partial^2 w}{\partial y^2}\right) + e_{31}\frac{\partial \varphi}{\partial z} + q_{31}\frac{\partial \psi}{\partial z}$$

$$\tau_{xy} = c_{66}\left(-z\frac{\partial^2 w}{\partial x\,\partial y} - z\frac{\partial^2 w}{\partial y\,\partial x}\right) = -2c_{66}z\frac{\partial^2 w}{\partial x\,\partial y} \tag{15}$$

$$D_z = e_{31}\frac{\partial u}{\partial x} + e_{31}\frac{\partial v}{\partial y} - \varepsilon_{33}\frac{\partial \varphi}{\partial z} - d_{33}\frac{\partial \psi}{\partial z} \tag{16}$$

$$B_z = q_{31}\frac{\partial u}{\partial x} + q_{31}\frac{\partial v}{\partial y} - d_{33}\frac{\partial \varphi}{\partial z} - \mu_{33}\frac{\partial \psi}{\partial z} \tag{17}$$

It should be noted that the components of the extended traction vectors in Ref. [2] are $[\sigma_{13}, \sigma_{23}, \sigma_{33}, D_3, B_3]^t$, which slightly differs from the present study but still represents the same physical meaning. Substituting Eqs. (16) and (17) into Eqs. (5) and (6), the following two algebraic equations can be easily derived:

$$e_{31}\frac{\partial}{\partial z}\left(-z\frac{\partial^2 w}{\partial x^2}\right) + e_{31}\frac{\partial}{\partial z}\left(-z\frac{\partial^2 w}{\partial y^2}\right) - \varepsilon_{33}\frac{\partial \phi}{\partial z} - d_{33}\frac{\partial \psi}{\partial z} = 0 \tag{18}$$

$$q_{31}\frac{\partial}{\partial z}\left(-z\frac{\partial^2 w}{\partial x^2}\right) + q_{31}\frac{\partial}{\partial z}\left(-z\frac{\partial^2 w}{\partial y^2}\right) - d_{33}\frac{\partial \phi}{\partial z} - \mu_{33}\frac{\partial \psi}{\partial z} = 0 \tag{19}$$

which also implies

$$-e_{31}\frac{\partial^2 w}{\partial x^2} - e_{31}\frac{\partial^2 w}{\partial y^2} - \varepsilon_{33}\frac{\partial^2 \phi}{\partial z^2} - d_{33}\frac{\partial^2 \psi}{\partial z^2} = 0 \tag{20}$$

$$-q_{31}\frac{\partial^2 w}{\partial x^2} - q_{31}\frac{\partial^2 w}{\partial y^2} - d_{33}\frac{\partial^2 \phi}{\partial z^2} - \mu_{33}\frac{\partial^2 \psi}{\partial z^2} = 0 \tag{21}$$

and can be rewritten as

$$\varepsilon_{33}\frac{\partial^2 \phi}{\partial z^2} + d_{33}\frac{\partial^2 \psi}{\partial z^2} = -e_{31}\left(\frac{\partial^2 w}{\partial x^2} + \frac{\partial^2 w}{\partial y^2}\right) \equiv -e_{31}\nabla^2 w \tag{22}$$

$$d_{33}\frac{\partial^2 \phi}{\partial z^2} + \mu_{33}\frac{\partial^2 \psi}{\partial z^2} = -q_{31}\left(\frac{\partial^2 w}{\partial x^2} + \frac{\partial^2 w}{\partial y^2}\right) \equiv -q_{31}\nabla^2 w \tag{23}$$

Thus, by adopting Crammer's rule, we may have

$$\frac{\partial^2 \phi}{\partial z^2} = -\frac{\Delta_1}{\Delta}\nabla^2 w \quad \text{and} \quad \frac{\partial^2 \psi}{\partial z^2} = -\frac{\Delta_2}{\Delta}\nabla^2 w \tag{24}$$

where

$$\Delta \equiv \det\begin{bmatrix} \varepsilon_{33} & d_{33} \\ d_{33} & \mu_{33} \end{bmatrix} \equiv \begin{vmatrix} \varepsilon_{33} & d_{33} \\ d_{33} & \mu_{33} \end{vmatrix} = \varepsilon_{33}\mu_{33} - d_{33}^2 \tag{25}$$

$$\Delta_1 \equiv \det\begin{bmatrix} e_{31} & d_{33} \\ q_{31} & \mu_{33} \end{bmatrix} = \begin{vmatrix} e_{31} & d_{33} \\ q_{31} & \mu_{33} \end{vmatrix} = (e_{31}\mu_{33} - d_{33}q_{31}) \tag{26}$$

and

$$\Delta_2 \equiv \det\begin{bmatrix} \varepsilon_{33} & e_{31} \\ d_{33} & q_{31} \end{bmatrix} = \begin{vmatrix} \varepsilon_{33} & e_{31} \\ d_{33} & q_{31} \end{vmatrix} = (\varepsilon_{33}q_{31} - d_{33}e_{31}) \tag{27}$$

It can be derived from Eq. (24) that

$$\frac{\partial \varphi}{\partial z} = -\frac{\Delta_1}{\Delta}z\nabla^2 w + \partial\varphi_0(x,y) \tag{28}$$

and

$$\frac{\partial \psi}{\partial z} = -\frac{\Delta_2}{\Delta}z\nabla^2 w + \partial\psi_0(x,y) \tag{29}$$

where $\partial\phi_0(x,y)$ and $\partial\psi_0(x,y)$ are functions that are independent of variable z, and can be treated as the variation of electric field and magnetic field in the thickness direction while the plate is vibrating and is obviously independent of z.

When a thin plate structure is under investigation, the following stress, moment, and shear force are well-defined

$$\begin{Bmatrix} N_x \\ N_y \\ N_{xy} \\ Q_x \\ Q_y \end{Bmatrix} = \int_{-h/2}^{+h/2} \begin{Bmatrix} \sigma_x \\ \sigma_y \\ \sigma_{xy} \\ \sigma_{xz} \\ \sigma_{yz} \end{Bmatrix} dz \tag{30}$$

$$\begin{Bmatrix} M_x \\ M_y \\ M_{xy} \end{Bmatrix} = \int_{-h/2}^{+h/2} \begin{Bmatrix} \sigma_x \\ \sigma_y \\ \sigma_{xy} \end{Bmatrix} z\,dz \tag{31}$$

After integrating Eqs. (30) and (31), with respect to the direction of plate thickness dz, five balance equations related the plate bending problem can be derived and stated as follows.

For force balance in x-direction,

$$\frac{\partial N_x}{\partial x} + \frac{\partial N_{yx}}{\partial y} + \tau_{1x} - \tau_{2x} = \rho_P h\frac{\partial^2 u}{\partial t^2}$$

For force balance in y-direction,

$$\frac{\partial N_{xy}}{\partial x} + \frac{\partial N_y}{\partial y} + \tau_{1y} - \tau_{2y} = \rho_P h\frac{\partial^2 v}{\partial t^2}$$

For force balance in z-direction,

$$\frac{\partial Q_x}{\partial x} + \frac{\partial Q_y}{\partial y} + p_1 - p_2 = \rho_P h\frac{\partial^2 w}{\partial t^2}$$

For moment balance in x-direction,

$$\frac{\partial M_x}{\partial x} + \frac{\partial M_{xy}}{\partial y} - Q_x + \frac{h}{2}[\tau_{1x} + \tau_{2x}] = 0$$

For moment balance in y-direction,

$$\frac{\partial M_{xy}}{\partial x} + \frac{\partial M_y}{\partial y} - Q_y + \frac{h}{2}[\tau_{1y} + \tau_{2y}] = 0$$

If there is no shear force on the surface (i.e., $\tau_{1x}=\tau_{2x}=\tau_{1y}=\tau_{2y}=0$), the balanced equations of a bending plate due to lateral load can be rewritten as

$$\frac{\partial M_{xy}}{\partial x} + \frac{\partial M_y}{\partial y} - Q_y = 0$$

$$\frac{\partial M_x}{\partial x} + \frac{\partial M_{xy}}{\partial y} - Q_x = 0$$

$$\frac{\partial Q_x}{\partial x} + \frac{\partial Q_y}{\partial y} + \Delta p(x,y) = \rho_P h \frac{\partial^2 w}{\partial t^2}$$

where $\Delta p(x,y) \equiv p_1(x,y) - p_2(x,y)$ represents the pressure difference between the upper and lower surfaces. Furthermore, the above three equations can be simplified into the following form:

$$\frac{\partial^2 M_x}{\partial x^2} + 2\frac{\partial^2 M_{xy}}{\partial x\,\partial y} + \frac{\partial^2 M_y}{\partial y^2} = -\Delta p(x,y) + \rho_P h \frac{\partial^2 w}{\partial t^2} \qquad (32)$$

Substituting Eqs. (28) and (29) into Eq. (15), and integrating them, with respect to the z-direction as shown in Eqs. (31), will lead to the following results:

$$\begin{aligned} M_x &= \int_{-h/2}^{h/2} \sigma_x z dz \\ &= \int_{-h/2}^{h/2} \left[c_{11}\left(-z\frac{\partial^2 w}{\partial x^2}\right) + c_{12}\left(-z\frac{\partial^2 w}{\partial y^2}\right) + e_{31}\left(-\frac{\Delta_1}{\Delta} z \nabla^2 w \right.\right. \\ &\quad \left.\left. + \partial \phi_0(x,y)\right) + q_{31}\left(-\frac{\Delta_2}{\Delta} z \nabla^2 w + \partial \psi_0(x,y)\right)\right] z dz \\ &= -\frac{h^3}{12}\left[c_{11}\frac{\partial^2 w}{\partial x^2} + c_{12}\frac{\partial^2 w}{\partial y^2} + e_{31}\frac{\Delta_1}{\Delta}\nabla^2 w + q_{31}\frac{\Delta_2}{\Delta}\nabla^2 w\right] \end{aligned} \qquad (33)$$

$$\begin{aligned} M_y = \int_{-h/2}^{h/2} \sigma_y z dz = -\frac{h^3}{12}\left[c_{12}\frac{\partial^2 w}{\partial x^2} + c_{11}\frac{\partial^2 w}{\partial y^2} + e_{31}\frac{\Delta_1}{\Delta}\nabla^2 w \right. \\ \left. + q_{31}\frac{\Delta_2}{\Delta}\nabla^2 w\right] \end{aligned} \qquad (34)$$

and

$$\begin{aligned} M_{xy} = \int_{-h/2}^{h/2} \sigma_{xy} z dz = \int_{-h/2}^{h/2} \tau_{xy} z dz = \int_{-h/2}^{h/2} c_{66}\left(-2z\frac{\partial^2 w}{\partial x\,\partial y}\right) z dz = \\ -\frac{h^3}{12}\cdot 2c_{66}\frac{\partial^2 w}{\partial x\,\partial y} \end{aligned} \qquad (35)$$

Substituting Eqs. (33) and (34) into Eq. (32) will result in the following expression for the bending problem of a MEE thin plate:

$$\begin{aligned} \frac{h^3}{12}\left\{ \frac{\partial^2}{\partial x^2}\left(c_{11}\frac{\partial^2}{\partial x^2} + c_{12}\frac{\partial^2}{\partial y^2} + e_{31}\frac{\Delta_1}{\Delta}\nabla^2 w + q_{31}\frac{\Delta_2}{\Delta}\nabla^2 w\right)\right. \\ + 4c_{66}\frac{\partial^2}{\partial x\,\partial y}\left(\frac{\partial^2 w}{\partial x\,\partial y}\right) + \frac{\partial^2}{\partial y^2}\left(c_{12}\frac{\partial^2}{\partial x^2} + c_{11}\frac{\partial^2}{\partial y^2} + e_{31}\frac{\Delta_1}{\Delta}\nabla^2 w \right. \\ \left.\left. + q_{31}\frac{\Delta_2}{\Delta}\nabla^2 w\right)\right\} = \Delta p(x,y) - \rho_P h\frac{\partial^2 w}{\partial t^2} \end{aligned} \qquad (36)$$

This also implies that

$$\begin{aligned} \frac{h^3}{12}\left\{ c_{11}\left(\frac{\partial^4 w}{\partial x^4} + \frac{\partial^2 w}{\partial y^2}\right) + c_{12}\left(2\frac{\partial^4 w}{\partial x^2\,\partial y^2}\right) + e_{31}\frac{\Delta_1}{\Delta}\nabla^4 w + q_{31}\frac{\Delta_2}{\Delta}\nabla^4 w \right. \\ \left. + 4c_{66}\frac{\partial^4 w}{\partial x^2\,\partial y^2}\right\} = \Delta p(x,y) - \rho_P h\frac{\partial^2 w}{\partial t^2} \end{aligned} \qquad (37)$$

and can be rewritten as

$$\begin{aligned} \frac{h^3}{12}\left\{ c_{11}\left(\frac{\partial^4 w}{\partial x^4} + \frac{\partial^2 w}{\partial y^2}\right) + 2(c_{12} + 2c_{66})\frac{\partial^4 w}{\partial x^2\,\partial y^2} + e_{31}\frac{\Delta_1}{\Delta}\nabla^4 w \right. \\ \left. + q_{31}\frac{\Delta_2}{\Delta}\nabla^4 w\right\} = \Delta p(x,y) - \rho_P h\frac{\partial^2 w}{\partial t^2} \end{aligned} \qquad (38)$$

where $\nabla^4 \equiv \nabla^2\nabla^2 \equiv \partial^4/\partial x^4 + 2(\partial^4/\partial x^2\,\partial y^2) + \partial^4/\partial y^4$. Since for a transversely isotropic material, the relation $c_{11}=c_{12}+2c_{66}$ holds, Eq. (38) can then be simplified into

$$\begin{aligned} \frac{h^3}{12}\left\{ c_{11}\left(\frac{\partial^4 w}{\partial x^4} + 2\frac{\partial^4 w}{\partial x^2\,\partial y^2} + \frac{\partial^2 w}{\partial y^2}\right) + e_{31}\frac{\Delta_1}{\Delta}\nabla^4 w + q_{31}\frac{\Delta_2}{\Delta}\nabla^4 w\right\} \\ = \Delta p(x,y) - \rho_P h\frac{\partial^2 w}{\partial t^2} \end{aligned} \qquad (39)$$

i.e., we can have

$$\frac{h^3}{12}\left\{ c_{11}\nabla^4 w + e_{31}\frac{\Delta_1}{\Delta}\nabla^4 w + q_{31}\frac{\Delta_2}{\Delta}\nabla^4 w\right\} = \Delta p(x,y) - \rho_P h\frac{\partial^2 w}{\partial t^2} \qquad (40)$$

Thus, the governing equation for a thin MEE bending plate is then derived as

$$\{D\nabla^4 w + E\nabla^4 w + M\nabla^4 w\} + \rho_P h\frac{\partial^2 w}{\partial t^2} = \Delta p(x,y) \qquad (41)$$

where $D \equiv c_{11}h^3/12$, $E \equiv e_{31}h^3/12\cdot\Delta_1/\Delta$, and $M \equiv q_{31}h^3/12\cdot\Delta_2/\Delta$ represents the plate rigidity, effective rigidities due to the presences of electricity, and magnetism, respectively.

3 Numerical Evaluations and Discussions

The free vibration analysis of the MEE plate are carried out by considering a bilayered $BaTiO_3$–$CoFe_2O_4$ composite with variable volume fraction (vf) of $BaTiO_3$. The density of the bilayer plate is assumed to be proportional to the volume faction of these two materials, i.e., $\rho_P = \rho_{BaTiO_3} * vf + \rho_{CoFe_2O_4} * (1 - vf)$. The study is conducted by choosing six different plates with volume fractions in steps of 20%, i.e., 0%, 20%, 40%, 60%, 80%, and 100%. The MEE material properties are listed in Table 1 with different volume fraction as given by Anandkumar [14]. It can be easily derived that the natural frequencies for the MEE thin plate with general boundary conditions governed by Eq. (41) are expressed as the following:

$$\omega_{mn}^2 = \frac{(D + E + M)}{\rho_P h}\cdot(\alpha_m^4 + 2\alpha_m^2\beta_n^2 + \beta_n^4) \qquad (42)$$

in which α_m and β_n are the corresponding eigenvalues according to the plate's boundary conditions along the x and y-directions, respectively. In this study, the MEE plate is assumed to be square, i.e., $L_x = L_y = L$. Nevertheless, all rectangular plates can be applied while adopting the frequency equation stated in Eq. (42).

Having the analytic solutions for the natural frequencies of MEE rectangular plates, we first apply Eq. (42) to the case of the purely elastic thin plate, aiming to validate the present analysis. For a purely elastic thin plate, it is obvious that the piezoelectric and piezomagnetic effects will vanish, i.e., $E \equiv 0$ and $M \equiv 0$. As a result, the equation will be reduced into a well-known thin plate frequency equation, and therefore directly verify the validity of the present study.

Second, a purely piezoelectric plate made of the commonly used PZT-4 material is proposed as the comparison between the

Table 1 Material constants for MEE $BaTiO_3$–$CoFe_2O_4$ composite (cited from Ref. [14])

vf	0%	20%	40%	60%	80%	100%
C_{11}	286	250	225	220	175	166
C_{12}	173	146	125	110	100	77
C_{13}	170	145	125	110	100	78
C_{33}	269.5	240	220	190	170	162
C_{44}	45.3	45	45	45	50	43
e_{31}	0	−2	−3	−3.5	−4	−4.4
e_{33}	0	4	7	11	14	18.6
e_{15}	0	0	0	0	0	11.6
ε_{11}	0.08	0.33	0.8	0.9	1.0	11.2
ε_{33}	0.093	2.5	5.0	7.5	10	12.6
μ_{11}	−5.9	−3.9	−2.5	−15	−0.8	0.05
μ_{33}	1.57	1.33	1.0	0.75	0.5	0.1
q_{31}	580	410	300	200	100	0
q_{33}	700	550	280	260	120	0
q_{15}	560	340	220	180	80	0
d_{11}	0	2.8	4.8	6.0	6.8	0
d_{33}	0	2000	2750	2500	1500	0
ρ_P	5300	5400	5500	5600	5700	5800

Unit: elastic constants C_{ij} in 10^9 N/m^2, piezoelectric constants e_{ij} in C/m^2, piezomagnetic constants q_{ij} in N/A m^2, dielectric constants ε_{ij} in 10^{-9} C^2/N m^2, magnetic constants μ_{ij} in 10^{-6} N s^2/C^2, and magnetoelectric coefficients d_{ij} in 10^{-12} N s/VC.

complete 3D analysis and the present 2D thin plate analysis in order to see the applicable range for the proposed methodology. The material constants for a PZT-4 ceramic plate are cited from Table 1 in Ref. [10], and the dimensions for the PZT-4 plate are chosen to be $h=0.05$ m for the thickness, $L_x=0.25$ m for the plate span in the x-axis, and $L_y=0.5$ for the one in the y-axis, respectively. It should be noted that the chosen dimensions are intended to fit the parameter requirements in Ref. [15], which was conducted by Chen et al., in which the length-to-width ratio $s_1 \equiv L_y/L_x$ is fixed at 2. Meanwhile, for the thin plate theory to be applicable, the thickness-to-span ratio $s_2 \equiv h/L_x$ is chosen to be 0.1. In their study, nondimensional natural frequencies for a piezoelectric rectangular plate are presented by adopting both the complete 3D state space method and the 2D plate theory, as shown in Fig. 2 of Ref. [15]. As we can detect from this figure, there are indeed huge differences between the 3D and 2D analysis, especially when the thickness-to-span ratio is getting larger. Nevertheless, some dimensionless frequencies are approximately extracted from this figure for both the 3D and 2D analysis in the case of $s_2=0.1$, and a comparison between these data and the results obtained by the proposed model is tabulated in Table 2. The nondimensional natural frequencies for the present study are formulated as $\Omega_{mn}=\omega_{mn}L_x\sqrt{\rho_P/C_{\max}}$, and are presented from first mode through third mode in order to describe the variations between 2D and 3D simulations. As we can see from Table 2, the nondimensional frequencies calculated by the present model are almost the same with the 2D analysis in Ref. [15], and the frequencies are always larger than the corresponding one obtained by the 3D theory; these phenomena also have been pointed out in Ref. [15].

As for the comparison with the existing MEE literatures, since most of the MEE plate analyses are performed in a complete 3D point of view, the results obtained by imposing the present 2D thin plate theory are quite different with those offered by the other research approaches such as in Refs. [4,9]. Although the dimensions for the MEE plate adopted in Refs. [4,9] do not actually ensure the thin plate theory requirement ($mH/L_x=nH/L_y\equiv 1$ and $H\equiv 0.3$ in both papers), two special cases on the nondimensional fundamental natural frequency for the MEE plates, the pure $BaTiO_3$ laminate, and the pure $CoFe_2O_4$ one are provided below with the dimensionless formula being $\Omega_{11}=\omega_{11}L_xL_y\sqrt{\rho_P/C_{\max}}/H$. The fundamental natural frequency by adopting the above dimensions for pure $BaTiO_3$ plate is 5.724, whereas the natural frequency for pure $BaTiO_3$ plate is 5.719. Even though the two data are far beyond the values presented in Ref. [4] ($\Omega_1=2.3$ for the pure $BaTiO_3$ case and $\Omega_1=1.9$ for pure $CoFe_2O_3$ case), the boundary conditions for the MEE plate on the top and bottom surfaces in Ref. [4] are set to be an open circuit, i.e., $D_z\equiv 0$ and $B_z\equiv 0$, which imposed two additional boundary conditions on the whole system; this might be one of the reasons why lower frequency in Ref. [4] was acquired. On the other hand, as it is stated

Table 2 Nondimensional natural frequencies for a PZT-4 rectangular plate

Nondimensional natural frequencies: $\Omega_{mn}=\omega_{mn}L_x\sqrt{\rho_P/C_{\max}}$	PZT-4: data chosen from Fig. 2 in Ref. [15]		$h=0.05$, $L_y=1$, $L_x=0.5$
Mode	3D	2D	Present
$m=1$, $n=1$	0.2	0.4	0.386
$m=1$, $n=2$	0.4	0.6	0.617
$m=1$, $n=3$	0.6	1	1.004
$m=2$, $n=1$	0.8	1.2	1.313
$m=2$, $n=2$	1.0	1.4	1.544
$m=2$, $n=3$	1.2	1.6	1.930

Table 3 Natural frequencies for a pure $CoFe_2O_4$ square plate (0% of $BaTiO_3$)

Omega (rad/s)	$m=1$	$m=2$	$m=3$	$m=4$	$m=5$
$n=1$	2100.8	5251.9	10,504	17,856	27,310
$n=2$		8403	13,655	21,008	30,461
$n=3$			18,907	26,260	35,713
$n=4$		Symmetry		33,612	43,066
$n=5$					52,519

Table 4 Natural frequencies for a bilayered square plate (20% of $BaTiO_3$)

Omega (rad/s)	$m=1$	$m=2$	$m=3$	$m=4$	$m=5$
$n=1$	2387.3	5968.3	11,937	20,292	31,035
$n=2$		9549.2	15,517	23,873	34,616
$n=3$			21,486	29,841	40,584
$n=4$		Symmetry		38,197	48,940
$n=5$					59,683

Table 5 Natural frequencies for a bilayered square plate (40% of $BaTiO_3$)

Omega (rad/s)	$m=1$	$m=2$	$m=3$	$m=4$	$m=5$
$n=1$	2166.2	5415.4	10,831	18,413	28,160
$n=2$		8664.7	14,080	21,662	31,410
$n=3$			19,496	27,077	36,825
$n=4$		Symmetry		34,659	44,407
$n=5$					54,154

Table 6 Natural frequencies for a bilayered square plate (60% of $BaTiO_3$)

Omega (rad/s)	$m=1$	$m=2$	$m=3$	$m=4$	$m=5$
$n=1$	1998.9	4997.3	9994.6	16,991	25,986
$n=2$		7995.7	12,993	19,989	28,984
$n=3$			17,990	24,986	33,982
$n=4$		Symmetry		31,983	40,978
$n=5$					49,973

Table 7 Natural frequencies for a bilayered square plate (80% of $BaTiO_3$)

Omega (rad/s)	$m=1$	$m=2$	$m=3$	$m=4$	$m=5$
$n=1$	1674.3	4185.8	8371.6	14,232	21,766
$n=2$		6697.3	10,883	16,743	24,278
$n=3$			15,069	20,929	28,463
$n=4$		Symmetry		26,789	34,324
$n=5$					41,858

Table 8 Natural frequencies for a pure $BaTiO_3$ square plate (100% of $BaTiO_3$)

Omega (rad/s)	$m=1$	$m=2$	$m=3$	$m=4$	$m=5$
$n=1$	1531.2632	3828.1581	7656.3162	13,015.7375	19,906.422
$n=2$		6125.0529	9953.211	15,312.6323	22,203.3169
$n=3$			13,781.3691	19,140.7904	26,031.475
$n=4$		Symmetry		24,500.2117	31,390.8963
$n=5$					38,281.5808

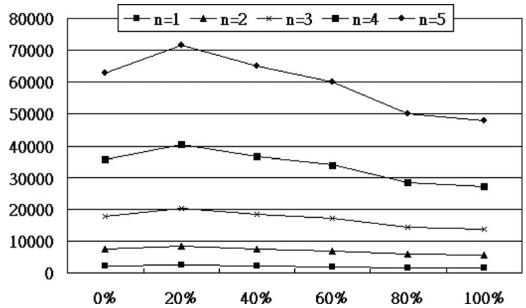

Fig. 1 Natural frequencies versus volume fractions of a MEE thin plate with various mode number (m=1)

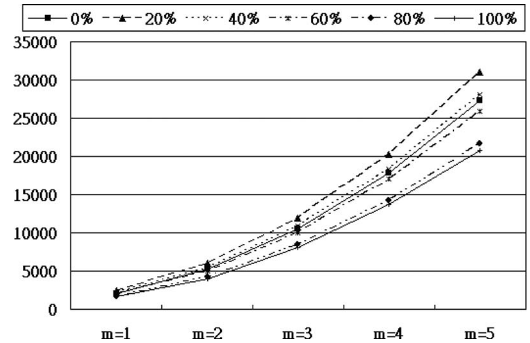

Fig. 2 Natural frequencies versus mode numbers for a MEE thin plate with various volume fractions (n=1)

in the last paragraph, the 2D analysis will always get a larger frequency than the 3D theory that has been concluded in Ref. [15].

Despite the overestimate on the natural frequencies caused by imposing the thin plate theory to the MEE laminate, the proposed model offers a simple, fast, efficient, and conservative prediction for the free vibration characteristic of a MEE rectangular bilayered thin plate provided by Eq. (42). Hereafter, the natural frequencies of the bilayered MEE thin plate, with different volume fractions of the PZ material $BaTiO_3$, will be investigated. Based on the classical thin plate theory, the ratio between thickness and spans of the plate should be less than 1:10. Therefore, the dimensions of the plate are assumed as follows: length $a=1$ m, width $b=1$ m, and height $h=0.05$ m; obviously, the dimensions adopted here suits the requirement. The boundary conditions for the MEE plate are chosen to be simply supported on four edges as an example, however, any kind of boundary conditions such as clamped end, free end, or a combination of these three boundaries can also be applied.

Tables 3–8 are the natural frequencies of the bilayered MEE thin plate that are subjected to different volume fractions of the PZ material $BaTiO_3$, which are ranging from 0% to 100%, with 20% offset. These tables are directly obtained by substituting the material parameters into the frequency equation, and it can be detected that, except for the pure PZ and PM material, the material parameter d_{11} and d_{33} are definitely not 0. Since d_{11} and d_{33} are the so-called magnetoelectric coefficients, which reveal the coupled effect between the PZ and PM phase when these two material are bonding together, the magnetoelectric interaction should be taken into account while a real MEE plate is under investigation.

In order to clearly watch the trend of variation for the natural frequencies of a bilayered MEE thin plate, some valuable data are selected from Tables 3–8, and rearranged as shown in Figs. 1 and 2. As it can be detected, the natural frequency of the MEE plate with 20% $BaTiO_3$ constituent always achieved the largest value in all five modes, whereas the deviation is not significant in the first two modes. Followed by the pure PM plate (i.e., 0% of $BaTiO_3$), the 40% case seems to be the second one, and then sequentially, the 60%, 80%, and 100% cases are placed in decreasing order. These phenomena are very interesting but also quite irregular; anyone dealing with the frequency problem of the related plates should pay attention to them.

Since the governing equation presented in Eq. (41) can be applied to any boundary conditions, two more examples for the boundary condition other than the simply-supported plate are added in the following equation. Table 9 shows the natural frequencies for the bilayered MEE square plates with clamped boundary conditions around four edges, whereas Table 10 presents the corresponding ones with clamped-free boundary conditions along the x- and y-axes. Due to the symmetry, with respect to the mode order m and n, only the upper diagonal results for orders

Table 9 Natural frequencies for MEE plate with clamped boundary conditions

Omega (rad/s)	0%	20%	40%	60%	80%	100%
ω_{11}	4762.19	5411.7532	4910.4804	4531.3201	3795.5025	3471.2023
ω_{12}	8944.6749	10,164.7295	9223.2042	8511.0391	7128.9756	6519.8524
ω_{13}	15,248.3328	17,328.207	15,723.1524	14,509.0971	12,153.0401	11,114.6442
ω_{22}	13,127.1599	14,917.7059	13,535.928	12,490.7582	10,462.4487	9568.5026
ω_{23}	19,430.8177	22,081.1834	20,035.8763	18,488.8162	15,486.5132	14,163.2944
ω_{33}	25,734.4756	29,244.6609	26,535.8245	24,486.8742	20,510.5777	18,758.0862

Table 10 Natural frequencies for MEE plate with clamped-free boundary conditions

Omega (rad/s)	0%	20%	40%	60%	80%	100%
ω_{11}	748.3894	850.4698	771.6936	712.1077	596.4722	545.5076
ω_{12}	2719.2329	3090.1365	2803.9074	2587.4051	2167.2498	1982.0728
ω_{13}	6940.3692	7887.0363	7156.4861	6603.9017	5531.5283	5058.8963
ω_{22}	4690.0764	5329.8033	4836.1212	4462.7025	3738.0274	3418.638
ω_{23}	8911.2126	10,126.703	9188.6999	8479.1991	7102.3059	6495.4615
ω_{33}	13,132.3489	14,923.6027	13,541.2787	12,495.6957	10,466.5844	9572.2849

ranging from 1 to 3 are presented. It can be easily verified that the fundamental natural frequency for the clamped-around plate is larger than that for the simply supported one, and followed by the result for the clamped-free case.

4 Conclusions

In this paper, the closed form expression for the transverse vibration of a MEE thin plate is derived, and the exact solution for the free vibration of a two-layered $BaTiO_3-CoFe_2O_4$ composite is obtained. The analytical solutions for the natural frequencies of the bilayered MEE thin plate that is subjected to different volume fractions of the piezoelectric material $BaTiO_3$, ranging from 0% to 100% with 20% offset, are presented. It can be concluded that the natural frequency of the MEE plate with 20% $BaTiO_3$ constituent will achieve the largest value in all five modes, whereas the deviation is not significant in the first two modes. The governing equation presented in this paper can be applied to any kind of boundary conditions such as simply-supported edge, clamped edge, free edge, or an arbitrary combination of them.

Acknowledgment

This work was partially supported by the National Science Council of Taiwan under Grant No. NSC-95-2211-E327-046. The authors are grateful for this support.

References

[1] Li, J. Y., 2000, "Magnetoelectroelastic Multi-Inclusion and Inhomogeneity and Their Applications in Composite Materials," Int. J. Eng. Sci., **38**, pp. 1993–2011.

[2] Pan, E., 2001, "Exact Solution for Simply Supported and Multilayered Magneto-Electro-Elastic Plates," ASME J. Appl. Mech., **68**, pp. 608–618.

[3] Aboudi, J., 2001, "Micromechanical Analysis of Fully Coupled Electro-Magneto-Thermal-Elastic Multiphase Composite," Smart Mater. Struct., **10**, pp. 867–877.

[4] Pan, E., and Heyliger, P. R., 2002, "Free Vibrations of Simply Supported and Multilayered Magneto-Electro-Elastic Plates," J. Sound Vib., **252**(3), pp. 429–442.

[5] Wang, X., and Shen, Y. P., 2002, "The General Solution of the Three-Dimensional Problems in Magnetoelectroelastic Media," Int. J. Eng. Sci., **40**(10), pp. 1069–1080.

[6] Chen, Z., Yu, S., Meng, L., and Lin, Y., 2002, "Effective Properties of Layered Magneto-Electro-Elastic Composites," Compos. Struct., **57**(1–4), pp. 177–182.

[7] Haojiang, D., and Aimin, J., 2004, "A Boundary Integral Formulation and Solution for 2D Problems in Magneto-Electro-Elastic Media," Comput. Struct., **82**, pp. 1599–1607.

[8] Guan, Q., and He, S.-R, 2005, "Two-Dimensional Analysis of Piezoelectric/Piezomagntic and Slastic Media," Compos. Struct., **69**, pp. 229–237.

[9] Chen, W. Q., Lee, K. Y., and Ding, H. J., 2005, "On Free Vibration of Non-Homogeneous Transversely Isotropic Magneto-Electro-Elastic Plates," J. Sound Vib., **279**, pp. 237–251.

[10] Ramirez, F., Heyliger, P. R., and Pan, E., 2006, "Free Vibration Response of Two-Dimensional Magneto-Electro-Elastic Laminated Plates," J. Sound Vib., **292**(3-5), pp. 626–644.

[11] Ugural, A. C., 1989, *Stresses in Plates and Shells*, Southeast Book Company, Taiwan.

[12] Tzou, H. S., "Piezoelectric Shells," *Distributed Sensing and Control of Continua*, Kluwer Academic Publishers, Netherlands.

[13] Gibson, R. F., 1994, *Principles of Composite Material Mechanics*, McGraw-Hill, New York.

[14] Annigeri, A. R., Ganesan, N., and Swarnamani, S., 2007, "Free Vibration Behavior of Multiphase and Layered Magneto-Electro-Elastic Beam," J. Sound Vib., **299**, pp. 44–63.

[15] Chen, W.-Q., Xu, R.-Q., and Ding, H.-J., 1998, "On Free Vibration of A Piezoelectric Composite Rectangular Plate," J. Sound Vib., **218**(4), pp. 741–748.